Chemolithotrophic microbial mats in an open pond in the continental subsurface – implications for microbial biosignatures

Christine Heim[1] *; Nadia-Valérie Quéric[1]; Danny Ionescu[2]; Klaus Simon[3] & Volker Thiel[1]

[1]*Department of Geobiology, Geoscience Centre, Georg-August University Göttingen, Goldschmidtstr. 3, 37077 Göttingen, Germany; Email: cheim@gwdg.de*
[2]*Max-Planck Institute for Marine Microbiology, Celsiusstr. 1, 28359 Bremen, Germany*
[3]*Department of Geochemistry, Geoscience Centre, Georg-August University Göttingen, Goldschmidtstr. 1, 37077 Göttingen, Germany*

* corresponding author

Göttingen Contributions to Geosciences
www.gzg.uni-goettingen.de

77: 99-112, 9 figs. 2014

The 450 m deep Äspö Hard Rock Laboratory (Äspö HRL), run by the Swedish Nuclear Fuel and Waste Management Co. (SKB) offers a unique opportunity to access microbial systems within Precambrian, mostly granodioritic rocks of the Baltic Shield. Biofilms and microbial mats at a deep groundwater seepage site and an associated pond exhibit a large diversity of aerobic and anaerobic, often chemolithotrophic microorganisms. An open pond system consisting of several different subsystems was studied to explore the diversity and spatial distribution of microbial communities and associated mineral precipitates. A further focus was placed on the establishment of inorganic biosignatures (especially trace and rare earth element (TREE) fractionation patterns) for biogeochemical processes involving subsurface microorganisms.

Received: 06 September 2013
Accepted: 06 January 2014

Subject Areas: Microbiology, Biogeochemistry, Geobiology

Keywords: Biosignatures, trace and rare earth elements, iron oxidizing bacteria, sulphate reducing bacteria, deep biosphere

Introduction

Biofilms cover almost every rock-water interface on Earth. Within biofilms and microbial mats, microorganisms often mediate (bio-)mineral formation due to their presence and metabolism that cause changes in the chemical equilibrium of the surrounding environment. While biologically induced mineralization pathways can be well specified in theory, they are often difficult to recognize and distinguish in natural samples. Nevertheless, such biogenic processes may produce minerals different from their inorganically formed varieties in shape, size, crystallinity, isotopic and trace element composition (Konhauser 1997; Ferris et al. 1999, 2000; Weiner & Dove 2003, Bazylinski et al. 2007; Haferburg & Kothe 2007; Takahashi et al. 2007; Templeton & Knowles 2009; Chan et al. 2011). Such inorganic 'biosignatures' may be specified and utilized for the identification of related biological processes in geological samples, even when organic biosignatures, namely lipid biomarkers, have not survived over geological time.

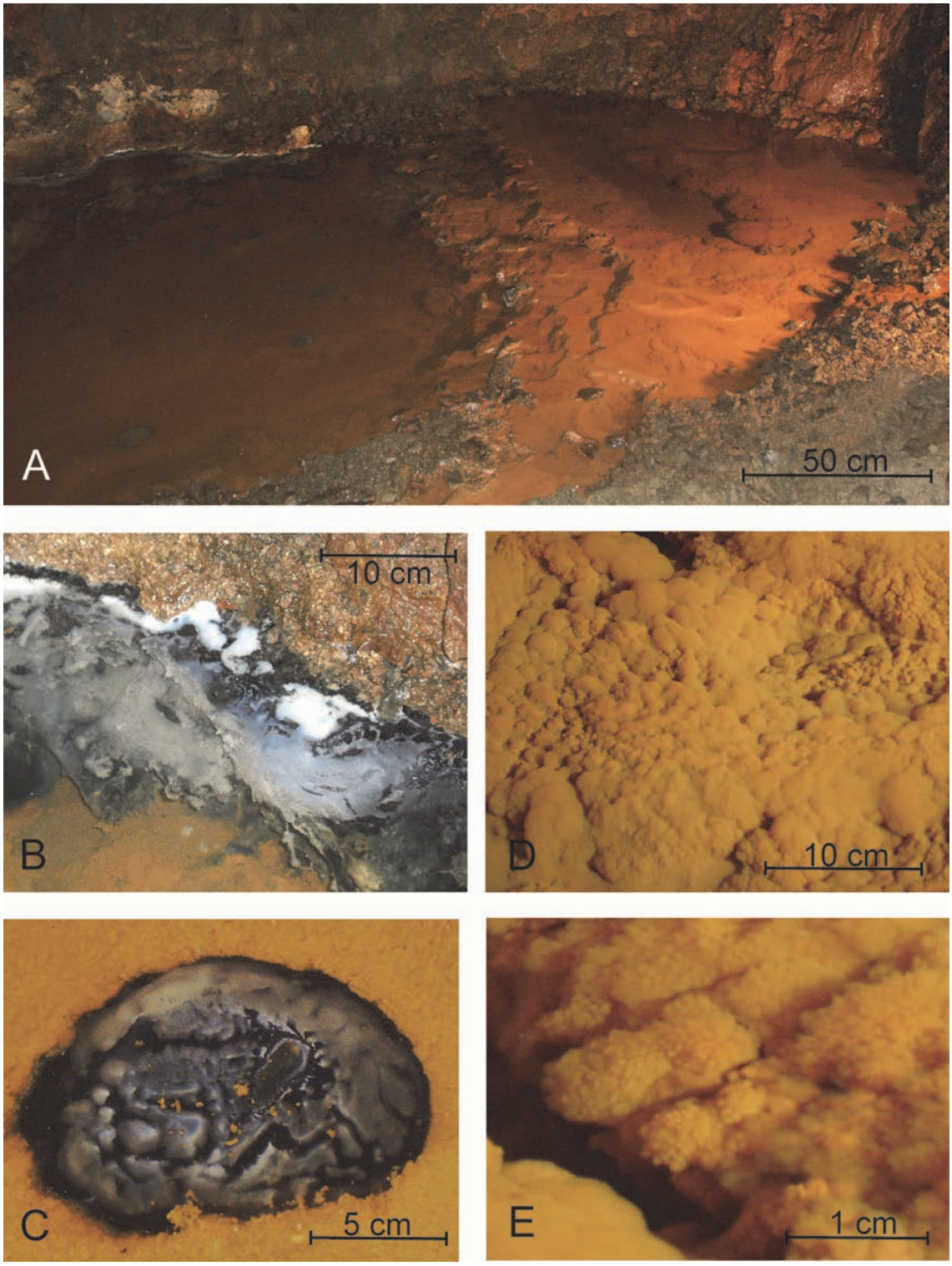

Fig. 1: The studied open pond at NASA 1127B in the Äspö HRL (**A**). The fluid inflow is located in the upper right corner and the outflow on the bottom left side (not visible). The ochre coloured, iron oxidizing microbial mats cover most of the pond area, whereas localized occurrences of white and black mats (**B, C**) are seen in the upper left corner. Details of ochre mat showing the internal cauliflower (**D**) and dendritic structures (**E**).

A better understanding of mineralizing microbial communities in the subsurface may furthermore provide insights and analogies to early Earth ecosystems. Early life on Earth probably developed in the subsurface, where it was protected from meteorite impacts and radiation penetrating the newly forming atmosphere (Trevors 2002; Russel 2003; Bailey et al. 2009).

In this study, mineralizing microbial mats were investigated from an open pond located at ca. 160 m depth in the Äspö Hard Rock Laboratory (HRL; north of Os-

karshamn, Sweden). The Äspö HRL was built as a testing environment for the disposal of nuclear waste and is operated by the Swedish Nuclear Fuel and Waste Management Co (SKB). In the Äspö HRL a wide spectrum of chiefly chemolithotrophically driven subsurface ecosystems is accessible (Pedersen 1997) that may offer a window into the microbial biosphere existing in continental vein systems. The study pond at the Äspö HRL site NASA 1127B (Fig. 1) exhibits a broad diversity of aerobic and anaerobic microorganisms, with iron/manganese oxidizing consortia forming a several cm thick microbial mat (Fig. 2). In our study, we paid particular attention to ion species involved in microbial mineralisation processes. To distinguish selective cation incorporation, three distinct types of microbial mats and the overlying water body were systematically analysed, and the in- and out-flows of the pond were compared. Especially trace and rare earth element (TREE) fractionation patterns were investigated to assess their potential utility as inorganic biosignatures for individual groups of microorganisms

Methods

Microbial mats

Microbial mats from the pond (Fig. 1A) were separated in three visually different mat types, (ochre, white and black). Whereas the ochre mat was mainly distributed over the whole pond, exhibiting a cauliflower structure (Figs. 1D, E), the black and the overlying white mat were contiguously distributed along the rim and at some localised spots in the pond (Figs. 1B, C). The mats were sampled with different devices, depending on the mat consistency, using spatulas, petri dishes and syringe cores. Additionally, an ochre mat core was taken with a plexiglas tube of 15 cm Ø and 25 cm length (Fig. 2). After sampling, the microbial mats were frozen, transported with dry ice, and stored at -20°C and -80°C (samples for DNA analysis) until further processing

Chemical analysis of the pond water and the microbial mats

Oxygen in the feeder fluids was measured using the Winkler method (Hansen 1999). Anion concentrations, measured by titration and ion chromatography, conductivity, pH and spectrophotometrical Fe_{total}/Fe(II) data were analysed immediately after sampling by the certified SKB chemistry lab.

For sample conservation and TREE measurements, concentrated, distilled HNO_3 was added to 50 ml water samples (final concentration 2 % HNO_3). In order to quantify the amounts of REE in the microbial mats, 4 ml of H_2O_2 and 2 ml of concentrated, distilled HNO_3*** were added to 500 mg of lyophilised sample. The resulting solutions containing the dissolved mineral precipitates were diluted in 50 ml of deionised water (final concentration 4 % HNO_3). These solutions, a reference sample (blank) containing all chemicals used, and the water samples were spiked with internal Ge, Rh, In and Re standards and analysed by ICP-MS and ICP-OES. As a reference, Fe_{total} was also measured by ICP-OES and was in good agreement with the spectrophotometrical data (1 % deviation). TREE were analysed using Inductive Coupled Plasma Mass Spectrometry (ICP-MS; Perkin Elmer SCIEX Elan DRCII) and Optical Emission Spectroscopy (ICP-OES; PerkinElmer Optima 3300 DV).

Carbon (C_{tot}), total nitrogen (N_{tot}) and sulphur (S_{tot}) were analysed using a CNS Elemental Analyser (HEKAtech Euro EA). C_{inorg} and organic carbon (C_{org}) were analysed with a Leco RC 412 multiphase carbon analyzer. Double measurements were performed routinely, and appropriate internal standards were used for the C_{inorg} (Leco 502-030), C_{org} (Leco 501-034), and CNS (BBot and atropine sulphate, IVA Analysentechnik SA990752 and SA990753) analyses.

Microsensor measurements

The microenvironment was probed using glass microsensors for O_2, pH and H_2S as previously described in (Santegoeds et al. 1998; Wieland et al. 2005). Four different environments were chosen for analysis: (1) Fresh looking ochre coloured mats in the upper part of the pond; (2) Aged mats of darker colour in the lower part of the pond; (3) Small black mat spots in the lower part of the pond; (4) Large black mat zone containing a white microbial mat in the corner of the lower part of the pond.

Fig. 2: Push core of an iron oxidizing microbial mat taken from the central part of the pond. The colour zoning and the different layers within the profile are attributed to different mat generations.

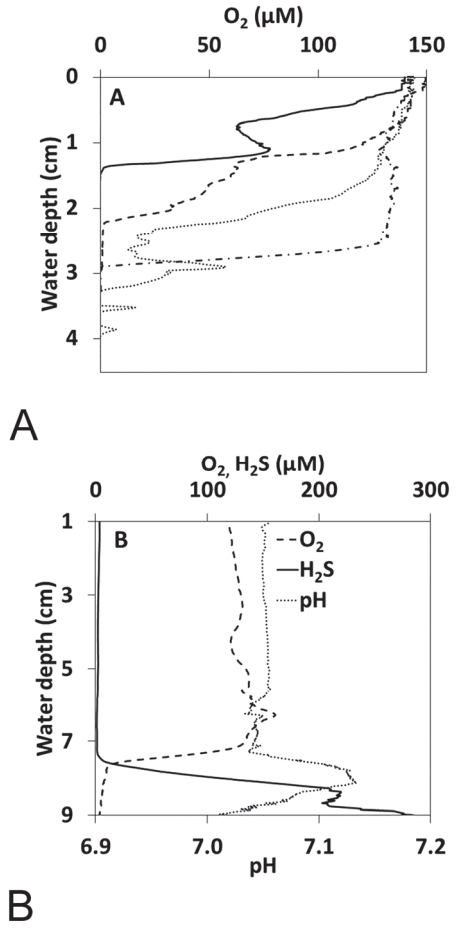

Fig. 3: Microsensor profiles into the ochre mat (**A**) and the black and white mat (**B**). The oxygen (O_2) concentration at different measurement points in the ochre mat decreases much faster in dense mat parts (continuous line) than in more fluffy mat parts (dashed lines, **A**). The O_2 and pH profiles penetrating the black and white mats show at first a roughly stable profile in the water column. At the mat surface (7 cm water depth) a sharp drop in O_2 concentration is visible, with a concurrent rise of the H_2S concentration and a pH shift by 0.1 (**B**).

Scanning Electron Microscopy and Energy Dispersive X-ray analysis (SEM-EDX)

For SEM-EDX analysis, the fresh samples were immediately fixed in 2 % glutardialdehyde and stored at 4°C until analysis. Prior to measurement, the samples were dehydrated in rising ethanol concentrations in 15 %, 30 %, 50 %, 70 % ethanol (30 min each), followed by 90 % and 99 % (60 min each), and 99 % ethanol (12 hrs). After the dehydration series, the samples were mounted on SEM sample holders and sputtered with Au-Pd (7.3 nm for 120 sec). Samples were analysed using a field emission SEM (LEO 1530 Gemini) combined with an INCA X-act EDX (Oxford Instruments).

Confocal Laser Scanning Microscopy (CLSM)

Structural characterization and localization of microbial cells and associated EPS structures within the mineralized ochre mats were examined by Laser Scanning Microscopy using a TCS SP1 confocal laser scanning microscope (Leica, Heidelberg, Germany).

Biofilm organisms were stained using nucleic acid-specific (Syto 9; Sybr Green) and protein-specific fluorochromes (Sypro Red). In addition, lectin-binding analysis was employed for the characterization of EPS glycoconjugates (PSA_Alexa568).

Fluorescence in situ *hybridization (FISH)*

Loosely attached microbial biofilms were carefully sampled by means of petridiscs with the aim to minimize biofilm destruction. Samples were fixed with 4 % paraformaldehyde (final concentration) for 4 hrs and carefully transferred to 1x PBS (10 mM sodium phosphate; 130 mM NaCl) three times before a final storage in 50 % ethanol/1x PBS at -20°C until further processing. Hybridization and microscopy visualisation of hybridized and 4-,6-diamidino-2-phenylindole (DAPI)-counterstained cells were performed as described previously (Snaidr et al. 1997). Cy3- and Oregon green monolabeled oligonucleotides were purchased from Metabion (Martinsried, Germany). Probes and formamide (FA) concentrations used in this study were as follows: EUB338 I-III targeting bacteria (Daims et al. 1999; 35 % FA), Non338 (negative control; Wallner et al. 1993; 10 % FA), Beta42 targeting Beta-Proteobacteria (Manz et al. 1992; 35 % FA), SRB385 targeting sulfate reducing bacteria (SRB) inclusive most species of the δ-group of purple bacteria (Amann et al., 1990; 35 % FA) and DSS658 targeting *Desulfosarcina* spp./*Desulfococcus* spp./*Desulfofrigus* spp. and *Desulfofaba* spp. (Manz et al. 1998; 35 % FA). Background signal of samples, observed with the nonsense probe NON338, was negligible (<0.1 %).

454 analysis

A DNA sample of the fresh looking ochre mat was sent for Roche 454 pyrosequencing at the MrDNA lab (Shallowater, TX, USA). Sequencing of the 16S rRNA gene was done using the 28F and 519R general primers (Lane 1991). 6500 sequences were obtained and were processed as described in Ionescu et al. (2012). Shortly, the sequences were checked for quality (length, homopolymers and ambiguous bases) and aligned against the SILVA ref database Sequences with poor alignment score were removed while the rest were dereplicated and clustered (per sample) into operational taxonomic units (OTUs) at a similarity value of 98 %. Reference sequences of each OTU were assigned to a taxonomy using BLAST against the SILVA ref database (Version 111; Quast et al. 2013). Full OTU mapping of the sample was done by clustering the reference sequences of each OTU at 99 % similarity.

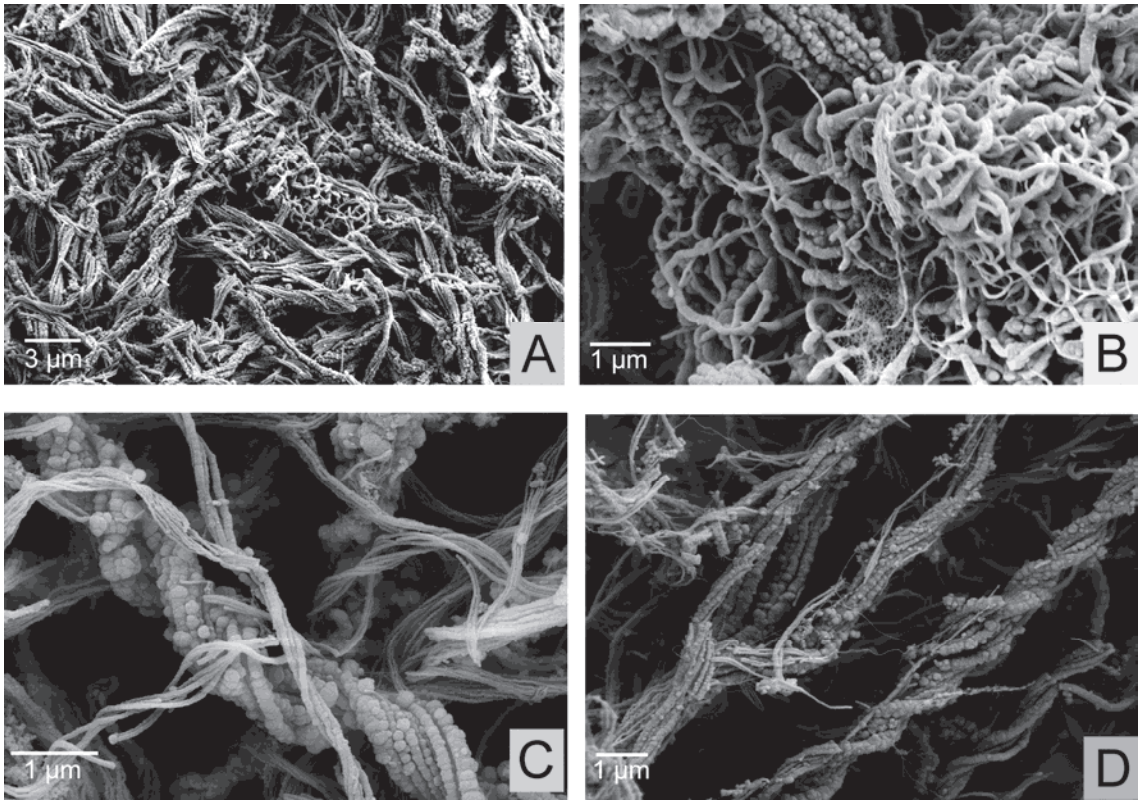

Fig. 4: SEM micrographs of the orange microbial mat, dominated by iron oxidizing bacteria (IOB). The microbial mat is visibly dominated by stalks produced by *Gallionella ferruginea* and *Mariprofundus* sp. (**A**). Iron oxyhydroxide precipitates resembling *Metallogenium*-like structures were occasionally observed (**B**). *Mariprofundus/Gallionella* EPS stalks show different stages of iron oxyhydroxide impregnation, most likely as a function of cell activity and age (**C**). The iron oxyhydroxide structures are connected via filigree structures similar to nanowires (**D**; Reguera et al. 2005).

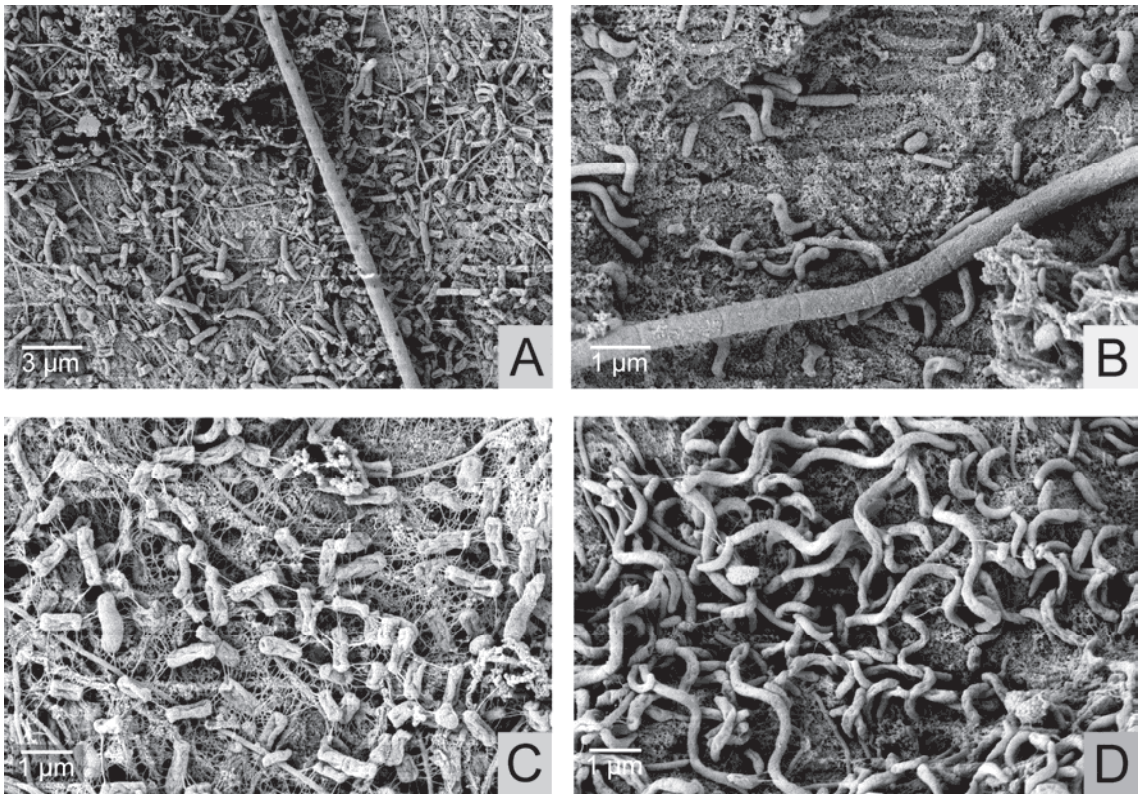

Fig. 5: SEM micrographs exhibiting different kinds of microbial cells and EPS structures of the white (**A**, **B**) and the black (**C**, **D**) microbial mats, mainly composed of rod shaped and spirally coiled cells; (**A**) rods, filaments, (**B**) rods, spirillum, (**C**) rods, (**D**) spirochaetes.

Table 1: Major physicochemical parameters of the pond water (NASA 1127B).

	1127B inlet	1127B main	1127B outlet
PO_4 µg/l	44.8	54.8	50.4
NO_3^-	1.9	2.7	11.0
pH	7.2	7.3	7.2
kond, mS/m	1090	1074	1075
Alkalinity, mg/l	184.8	173.9	168.6
Uranine, %	0.2	0.2	0.2
Cl, mg/l	3461	3405	3409
Br mg/l	15.8	15.2	14.5
SO_4 mg/l	333.6	346.3	346.5
F mg/l	1.8	1.8	1.8
Ca mg/l	374.0	346.7	347.9
Na mg/l	1521	1511	1537
Mg mg/l	141.4	143.4	145.1
K mg/l	38.0	40.3	40.5
Fe tot mg/l	1.59	0.3	0.3
Fe(II) mg/l	1.51	0.3	0.1
Mn mg/l	0.8	0.8	0.8
Al mg/l	0.1	0.3	0.1
Sr mg/l	6.7	6.2	6.2
Ba mg/l	0.1	0.1	0.1
Si mg/l	4.5	4.3	4.3
O_2 mg/l	0.7	1.6	1.9
H_2S mg/l	0.04	0.08	0.02

DNA extraction, PCR amplification and Denaturing Gradient Gel Electrophoresis (DGGE)

Genomic DNA was extracted directly from environmental subsamples by using the Ultra Clean Soil DNA extraction kit (MOBIO Laboratories, Inc., CA) according to the manufacturer's protocol.

Partial 16S rRNA gene amplification from environmental DNAs for subsequent DGGE-analysis was performed using the primer sets GM5F (341F) with a GC clamp and 907R for bacteria (Muyzer et al. 1995), ARC344F-GC and 915R for archaea (Casamayor et al. 2000) as well as DSRp2060F-GC (Geets et al. 2006) and DSR4R (Wagner et al. 1998) targeting sulphate reducing bacteria, following the respective PCR protocols of the former authors. PCR products in an amount ranging from 300 to 500 ng was applied to DGGE as described by Schäfer & Muyzer (2001), using the D-Code system (Bio-Rad Laboratories, CA). Electrophoresis was performed with 6 % polyacryl-amide gels (ratio of acrylamide to bisacrylamide, 40:1) submerged in 0.75 x TAE buffer (40 mM Tris, 40 mM acetic acid, 1 mM EDTA, pH 7.5) at 60°C and run for 16 hrs at 100 V in a linear 20 to 70 % denaturant gradient. Stained with ethidium bromide (0.5 g/ml), individual bands were excised and re-suspended overnight at 4°C in 50 µl of Milli-Q water. After re-amplification with the original primer sets, PCR products were purified via the Qiaquick PCR purification kit (QIAGEN GmbH, Hilden, Germany) prior to direct sequencing by using an ABI Prism 3100 genetic analyser (PE Applied Biosystems).

The partial 16S rRNA sequences were assembled and manually corrected using the BioEdit sequence alignment editor (Hall 1999), and further compared to the Gen-Bank database by the BLAST analysis tools of the National Centre for Biotechnology Information (Altschul et al. 1990) in order to determine their phylogenetic affiliation and to identify their closest phylogenetic relatives.

The deduced, partial dsrB sequences of the environmental samples were implemented into the persisting dsrAB alignment of SRP references strains, including all full-length Dsr sequences available from the public databases. The data sets were phylogenetically analysed with the tree inference methods included in the ARB software package (Ludwig et al. 2004) and the Phylogeny Inference Package Version (PHYLIP) 3.5c (Felsenstein 1993).

Results

Water chemistry

Water chemistry data are given in Tables 1 and 2B. Our three-years-monitoring of the pond water chemistry did not reveal any extensive seasonal variation or other fluctuation. Therefore, data given in Table 1 and 2B are mean values of five sampling time points. Chemical variations observed between the inlet, main pond and outlet are rather small (Table 1). The concentration of dissolved iron (FeII) at the inlet (1.6 mg/l) is almost completely consumed in the pond (outlet: 0.1 mg/l). Alkalinity drops from 184.8 mg/l to 168.6 mg/l as does Ca^{2+} from 374 mg/l to 348 mg/l. On the other hand, the concentrations of PO_4^{3-} (44.8 mg/l), NO_3^- (1.9 mg/l), and SO_4^{2-} (333.6 mg/l) increase to 50.4 mg/l, 11.0 mg/l, and 346.5 mg/l, respectively. The oxygen (O_2) concentration in the water column varies between 1.2–4.8 mg/l (37–150 µmol/l), but closer to the mat surfaces the O_2 concentration rises from the 0.7 mg (21.1 mmol/l) at the inlet to 1.9 mg (58.0 mmol/l) at the outlet. Oxygen profiles starting at the water surface into the ochre mats (at 1 cm water depth) show a clear decrease in oxygen concentration (Fig. 3A). The decline depends on the density of the ochre mat. The fluffy nature of the mats is clear from the intrusion of water with a higher O_2 content to deeper parts in the mats. The oxygen consumption alters between the different layer of the mat and is much slower in the upper fluffy part than in the denser deeper parts. O_2 and pH profiles down into the white and black mat show a roughly stable water column above these mats, and a sharp drop in O_2 concentration at the mat surface (7 cm water depth). Concurrently the H_2S concentration rises significantly and the pH is shifted by 0.1 (Fig. 3B).

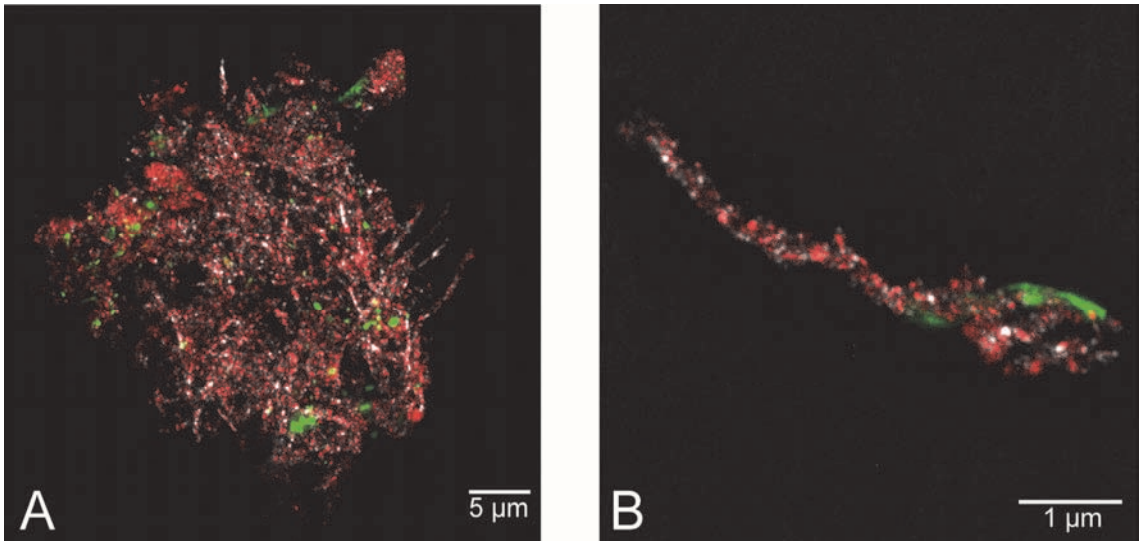

Fig. 6: Laser scanning microscopy (CLSM) of an ochre microbial mat. Fluorescence lectin-binding analysis was performed using nucleic acid and protein-specific fluorochromes (green) as well as the D-glucose and D-mannose staining lectin (red). Mineral precipitates are visible as white reflections. In the mat aggregate, a clear recognition of cells and their relation to appending stalks was impossible (**A**). In a partly mineral impregnated stalk fragment a smooth protein end was detected (**B**).

Table 2A: Major cation concentrations in the microbial mats. The thick ochre mats were analysed in three different sections (each 7cm), in order to check for potential stratifications.

g/kg	White mat	Black mat	Ochre core top	Ochre core middle	Ochre core bottom
Al	2.469	6.200	0.025	0.027	0.063
Ca	29.5	56.3	13.9	16.1	13.4
Cr	0.024	0.016	0.002	0.003	0.003
Fe	60.3	76.7	150.3	154.0	143.4
K	1.66	2.35	0.137	0.204	0.155
Mg	7.85	10.30	1.19	1.42	1.11
Mn	0.295	0.469	4.17	6.25	5.60
Na	53.6	30.8	5.49	7.97	4.46
Sr	0.326	0.368	0.473	0.567	0.489
Ti	0.678	1.629	0.003	0.004	0.010
Si	7.05	13.71	16.10	18.42	17.77

Microbial mat structure and community

The different mat types differ significantly in their content of organic matter. The ochre mat contains 5.1 to 5.8 % C_{org} (organic carbon), the black mat 15.4 % C_{org} and the white mat 17.6 % C_{org}.

Whereas the ochre mat consists mainly of iron oxyhydroxide impregnated stalks produced by iron oxidizing bacteria (IOB), numerous bacterial cells and EPS structures are visible in the black and white mat (SEM images, Figs. 4, 5). CLSM images from the lectine-stained ochre mat show a diffuse network of mineralized stalks without a clear relation to the stalk-producing cells (Fig. 6A). Some stalk fragments contained a non-encrusted protein band of unclear function (Fig. 6B).

The community compositions of the microbial mat at the inlet, outlet and in the main pond, respectively, were analysed by FISH, 16S rRNA gene analyses, and by 454 pyrosequencing. 454 pyrosequencing of the ochre mat resulted in 6500 sequences per sample, allowing a good overview of the large diversity of iron-oxidizing (depositing) bacteria. Among the identified genera were *Gallionella, Sideroxydans, Crenothrix, Marinobacter, Acidithiobacillus, Thiobacillus, Acidovorax*, a large diversity of Hyphomicrobiaceae including *Pedomicrobium, Filomicrobium*, and the recently isolated marine iron oxidizing bacterium *Mariprofundus* (Emerson et al. 2007) that dominated this environment. Although an initial clone library (data not shown) several sequences were related to known *Leptothrix* sequences none could be detected in the 454 sequences.

In comparision to sequences published in the International Nucleotide Sequence Database GenBank (in the following, accession codes are put in parentheses), sequences obtained by DGGE band excision and re-amplification inter alia showed high similarities to two alpha-proteobacteria: a mucus bacterium (AY654810.2) and *Citreicella thiooxidans* (AY639887.1), a lithoheterotrophic sulphur-oxidizing bacterium, which had been detected at first in the Black Sea (Sorokin et al. 2005). The ochre microbial mats also harboured the beta-proteobacterium *Nitrosomonas sp.* (AB113603.2, AJ275891.2) and *Thiocapsa sp.*

(AJ632077.2), a sulphur-oxidizing delta-proteobacterium. The sulphate-reducing bacteria, *Desulfolobus propionicus* (AY953411.1, AY354098.1, AY354099.1, AY953400.1, DQ250787.1, AY953399.1), *Desulfolobus rhabdoformis* (AB263181.1, DQ250778.1), *Desulfobacterium autotrophicum* (AB263151.1) and *Desulfotalea psychrophila* (AY354094.1) were found in all mat types (white, black and ochre). DGGE-derived sequences with high similarity to *Methylomonas sp* (EF212354.1, AY424847.1, AY550695.1) were found in both ochre mat consortia connected to in- and outlet, as well as in white and black mats. Only two out of six archaeal species present in the ochre mat types could be blasted (NCBI, Blastx) yet, one with an uncultured Crenarchaeote (AF201358.1) and one with a ferromanganous micronodule archeon (AF293019).

FISH was used to illustrate the relation between the autotrophic denitrifying *Thiobacillus denitrificans* and sulphate reducing bacteria by comparing the white and black mats, applying according probe combinations (Fig. 7). Both community compounds were densely packed, dominating within the white mat, while the underlying black mat aggregation was dominated by SRB, but also interspersed with minerals and bacteria other than beta-proteobacteria, as shown by pure DAPI signals (Figs. 7B-C)

Microbial mat chemistry

Microscopy and LA-ICP-MS were used to investigate TREE fractionations and accumulations within the different microbial mats. A distinctive TREE pattern of each mat type, if existing, can potentially serve as an inorganic biosignature for iron oxidizing, sulphate reducing bacteria and sulphur oxidizing bacteria (IOB, SRB, SOX) respectively. Major and trace element contents of the microbial mats are given in Tables 2A and 2B. In the ochre mat, Fe, Mn, and Si are considerably more abundant than in the white and black mats. These elements seem to be distributed evenly within the ochre mat as our analyses did not reveal any element accumulation in a particular zone of the mat profile (Table 2A; see also Fig. 2).

On the other hand, in the white and black mats, alkaline and alkaline earth metals (Ca, K, Mg, Na) and the elements Al, Cr and Ti are significantly enriched as compared to the ochre mat (Table 2A). In all microbial mat types, REE were enriched up to 10^4-fold compared to the pond water (Table 2B). Whereas some transition metals (Sc, V, Cr, Co) do not show significant accumulation in any of the microbial mats, other transition metals (Cu, Zn), as well as the elements Se, As, Rb, Cs, Cd, Mo, Bi are highly enriched in the black and white mat (Tables 2A-B).

When normalising the observed element accumulation patterns on the pond water, it is possible to distinguish individual fractionation behaviours of the different mat types. Fig. 9 shows the accumulation of individual elements in order of increasing enrichment.

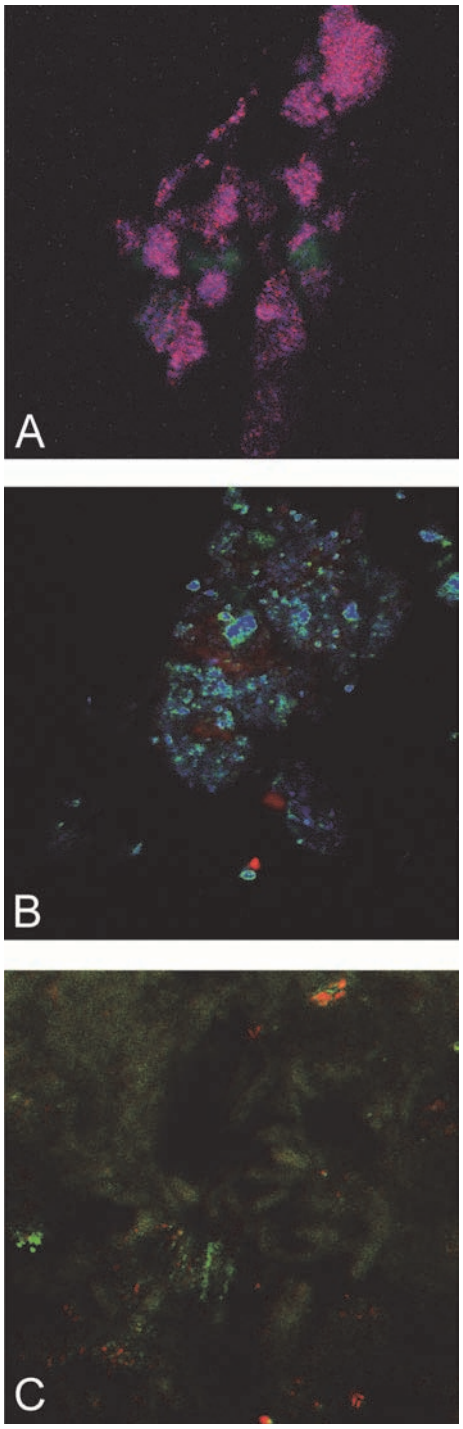

Fig. 7: Laser scanning microscopy coupled with fluorescent *in situ* hybridization (FISH) applying probes Beta42_og (Beta-proteobacteria, labeled with oregon green) and DSS658(cy3) (*Desulfosarcina/Desulfococcus*) on white consortia (**A**); Beta42(cy3) and SRB385(og) (sulfate reducing bacteria) applied to the black mat (**B, C**) from the main pond (abbreviations for fluorochromes cyanine 3 and oregon green in parentheses).

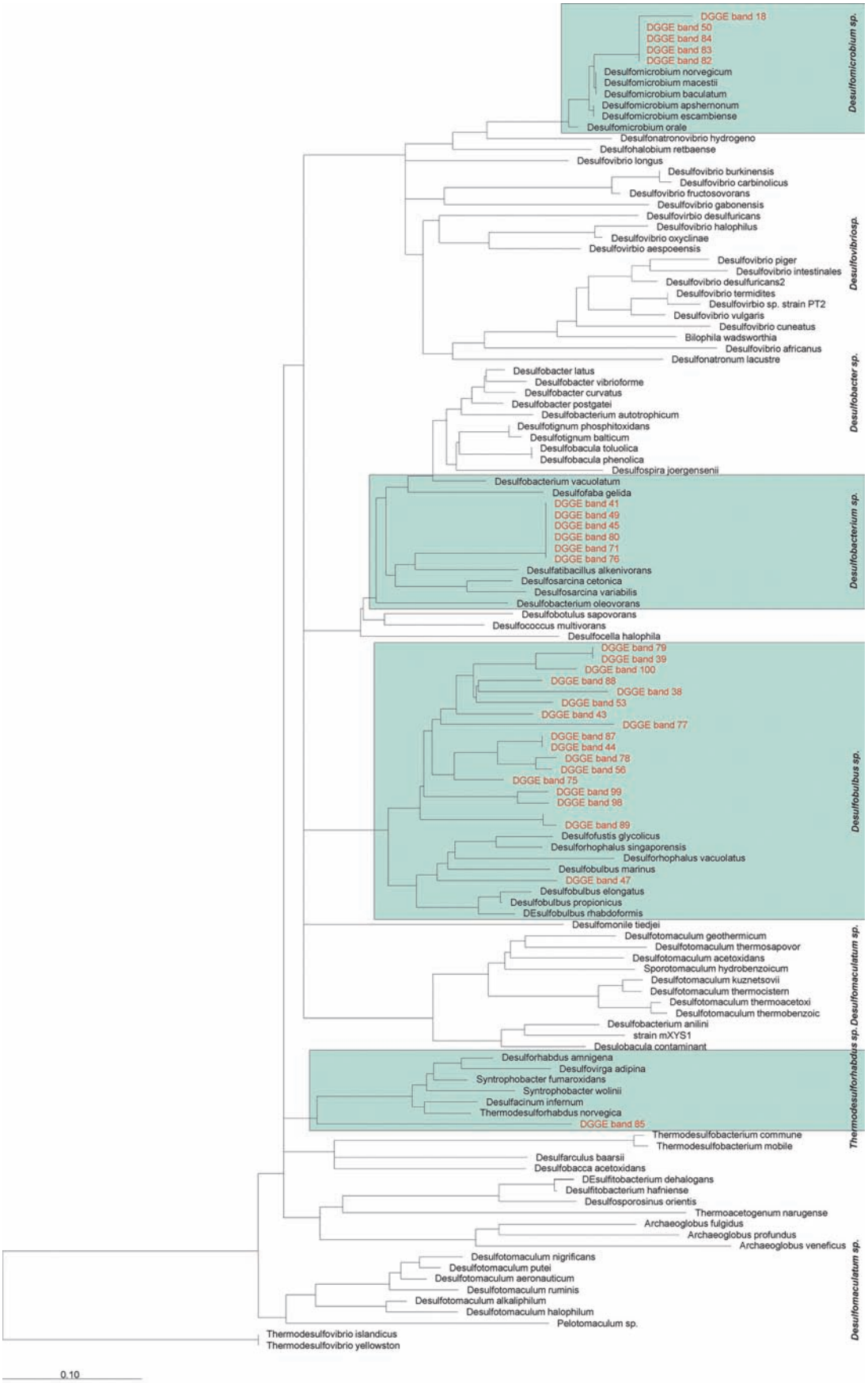

Fig. 8: Fitch-Margoliash tree (Consensus) of re-amplified DGGE-bands based on dsrB-derived PCR-products, indicating the encoding gene for the dissimilatory sulfate reductase. Areas indicate similarities to species matched by BLASTx (NCBI).

Table 2B: Trace element concentrations from the main pond water and from the black, white and ochre mats, respectively. TREE showed an even distribution along the ochre-mat profile, therefore, the data from this profile were merged (Table 2B) [b.d. = below detection limit].

	Pond water mean mg/l	Ochre mat mg/kg	White Mat mg/kg	Black mat mg/kg
Li	155.7	35.43	342	193.4
Be	0.04	134.66	5.3	7.7
Sc	14.66	1283	b.d.	b.d.
V	78.7	272.35	246.8	224.3
Co	3.95	14.60	24.5	52.2
Ni	55.25	43.06	85.2	202.2
Cu	4.32	39.47	141	354
Zn	6.99	76.04	363	543
As	33.0	16.35	85.1	36.2
Se	13.1	4.69	51.3	17.3
Y	0.31	891	116	155
Zr	0.17	381	60.3	90.3
Nb	0.04	10.56	8.3	24.6
Mo	2.45	75.6	387	735
Cd	0.01	0.18	1.4	1.8
Sn	b.d.	2.49	12.9	27.0
Sb	0.16	0.77	1.8	2.0
Rb	48.1	25.8	75.9	166
Cs	5.43	3.26	101.2	91.8
Ba	1331	61457	977	1974
La	0.06	257.0	102.2	231.6
Ce	0.06	357	174.8	420
Pr	0.01	44.9	20.8	46.8
Nd	0.11	209.3	83.3	176.0
Sm	0.01	40.4	bd	4.32
Eu	b.d.	6.96	2.15	4.89
Gd	0.02	74.50	15.0	26.3
Tb	0.002	9.48	1.68	3.03
Dy	0.02	75.3	12.7	18.8
Ho	0.005	22.3	3.35	4.41
Er	0.02	80.6	9.86	12.7
Tm	0.003	11.5	1.43	1.97
Yb	0.03	84.4	9.64	13.5
Lu	0.01	16.7	1.95	2.45
Hf	0.001	1.33	1.01	1.74
Ta	b.d.	0.02	0.63	1.31
W	0.39	302	47.3	63.1
Tl	b.d.	0.11	0.33	0.85
Pb	b.d.	59.30	79.2	158.7
Bi	b.d.	0.24	1.01	2.81
Th	b.d.	2.56	18.4	26.3
U	1.28	21.82	21.1	39.3

Comparing the black and white mat, they show a similar fractionation pattern, but rather contrasting to the ochre mat. The white and black mats show a generally higher enrichment of most of the trace elements except for the REE. The highest REE accumulation rates were observed in the ochre mat. Furthermore, the even fractionation pattern shows that the REE distribution of the ochre mat mirrors quite exactly the major water chemistry, but with an enrichment factor of about 10^4. The white and black mats show a preferential enrichment of the light REE (La-Sm) over the heavy REE (Gd-Lu).

Discussion

The water chemistry of the pond remained quite stable over the three years, and no seasonal variations were detected. The interaction between the microbial mats and the pond water seem to be rather stable. A remarkable impact of the microbial mat activity on the pond fluid is the maintenance of hypoxic conditions close to the mats (Table 1), even though the large pond surface is exposed to a "normal" atmosphere. Although the oxygen concentration of the pond water is significantly higher close to the pond surface, the microbial community of the ochre mat seems to be able to maintain favouring conditions to oxidize Fe(II). Keeping the O_2 concentration below 5 mg/l (ca. 150 µmol/l) in the main pond water enables a half life time of Fe(II) of several minutes (Emerson et al. 2010 and references therein). These conditions still allow iron oxidizing microbial communities to thrive and form thick microbial mats all over the pond.

The pyrosequencing results indicate that *Gallionella* sp. is not as abundant in the ochre mat as it was anticipated from previous reports (Pedersen & Hallbeck 1985; Hallbeck et al. 1993; Pedersen et al. 1996; Anderson & Pederson 2003). Rather, *Mariprofundus ferrooxidans* was found to be the dominating stalk-producing IOB in the studied pond. Although a visual differentiation through comparison of the order and structures of the stalks between certain *Gallionella* and *Mariprofundus* species is possible (Comolli et al. 2011), such differences where not observed in our samples. Both *G. ferruginea* and *M. ferrooxidans* are able to cast off their old, mineral-covered stalks and replace them by fresh ones (Cholodny 1926; Emerson et al. 2007). Due to the effective production of iron oxyhydroxides and the permanent replacement of heavily encrusted stalks, the ratio of mineral precipitates to organic matter is extremely high in these IOB-dominated mats.

The TREE accumulation in the ochre mat shows a signature, conserving mostly the TREE pattern of the feeder fluid, especially the REE (Fig. 9) with a constant 10^4 enrichment. The iron oxidizing bacteria *Mariprofundus* sp. and *G. ferruginea* are able to control the iron mineralization process to some degree (Saini & Chan 2012). This would allow a localized distribution of the biotic and abiotic minerals formed. Although the stalk surface is smooth and pristine during the initial stage of formation, with increasing distance and age, the stalk becomes more and more coated with lepidocrocite (FeOOH) and two-line ferrihydrite (Chan et al. 2011).

The accumulation rates of REE, Be, Y, Zr, Nb, Hf and W in the ochre mat were as high as those of Fe (Tables 2A-B) indicating a co-precipitation with the iron oxyhydroxides. This strong metal sorption capacity of iron oxyhydroxides is also widely used in technical applications and remediation activities (de Carlo et al. 1998; Bau 1999; Cornell & Schwertmann 2004; Michel et al. 2007).

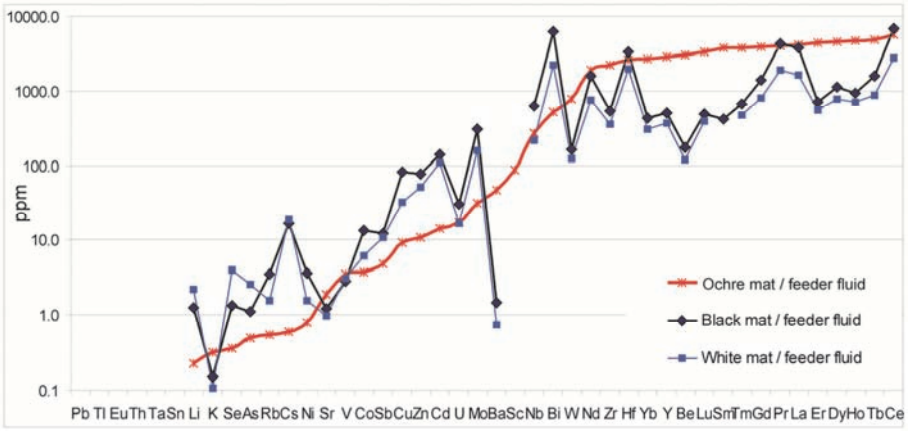

Fig. 9: Element fractionation in mineralized microbial mats normalised on the inflowing water. All data are mean values of five single samples from the same mat type. The elements are ordered according to the highest accumulation in the ochre mat. All microbial mat types (ochre, black and white) show an up to 10^6 fold accumulation of TREE compared to the TREE content in the aquifer. In addition, the TREE pattern ochre mat resembles quite exactly the pattern of the feeder fluid, whereas the black and white mats show more distinctive fractionations.

However, not only the microbial iron oxyhydroxides, but also the EPS-composed stalks play an important role in TREE precipitation as they offer large reactive surfaces for the biosorption of metals. Metals with a higher positive charge tend to show enhanced biosorption (Haferburg et al. 2007). This may also explain the higher enrichments observed for the 3- and 4-valent elements Si, Mn, REE, Y, Zr, Hf, U, and W compared to lower valent elements like Ca, K, Mg, Na, Cs, Rb and Li. However, although a preferential uptake of specific elements was not observed in the IOB dominated ochre mat, the general enrichment pattern seems to reflect the environmental conditions throughout the activity of the microbial mat.

According to DGGE as well as FISH results, the black and white mats seem to harbour similar community members mainly involved in sulphur oxidation, autotrophic denitrification, aerobic methylotrophy and sulphate reduction, which have been shown to build layers of dense aggregates (Fig. 6). Sulphur compounds are both used by SRB and autotrophic denitrifiers such as *Thiobacillus denitrificans* as electron donor, coupling the oxidation of inorganic sulphur compounds (such as hydrogen sulphide and thiosulphate) to the reduction of oxidized nitrogen compounds (such as nitrate, nitrite) to dinitrogen. This facultative anaerobic beta-proteobacterium was found also to couple the anaerobic oxidation of Fe(II) to denitrification, utilizing poorly-soluble minerals containing reduced iron and/or sulphur, such as pyrite (FeS_2) and FeS (Straub et al. 1996).

Overall, sulphate reducers are found in all type of mats presented here, while not all of them exhibited an active dissimilatory sulphate reduction; such, most sequences obtained by DGGE on the base of functional genes such as dsrB (Fig. 8) fall within the *Desulfobacterium* sp., *Desulfobulbus* sp. and *Desulfomicrobium* sp. clusters. However, any similarity to *Desulfobulbus* sp. might overlap with *Desulfocapsa* sp., which was not included in this analysis. Despite their visual appearance, the microbial communities of the black and the white mat were rather similar, harbouring a significant amount of SRB, closely aggregated with beta-proteobacteria such as *Thiobacillus denitrificans* (Fig. 7). This is in good agreement with H_2S profiles (Fig. 3), in the white and black mat, showing a high concentration above the black mat and decreasing in the white mat. Although SEM analyses indicate the presence of filamentous, sulphur-oxidizing bacteria (Fig. 5), no respective sequences could be retrieved from DGGE band sequencing. In general, fingerprinting analyses need always careful interpretation, including the evaluation of bias of PCR primer-based strategies (Mahmood et al. 2006) and the fact of potentially poor amplicon separation by DGGE and re-amplification (Nikolausz et al. 2005). Consequently, the total of sequences obtained by DGGE band excision may not represent all members of the complete microbial community in the pond

Although a great similarity between the microbial communities at the in- and outflow were detected the localized occurrence of specialized mat types in the pond argues for different controlling factors for the microbial mat formation. The substrate could be such a controlling factor. Indeed, the analysis of rock samples showed that at the growth location of the black and white mats, the surrounding grano-dioritic host rock was covered with concrete. Apparently, the presence of concrete created a micro-environment within the pond that favoured the presence of SRB and SOX communities. Concretes and cements commonly contain considerable amounts of either gypsum or sulphate rich fly ash (e.g., Iglesias et al. 1999; Guo & Shi 2008; Camarini & De Milito 2011). Thus, the concrete may serve as a likely sulphate source for the microbial communities.

The high accumulation of Cu, Zn, Se, As, Rb, Cs, Cd, Mo, Bi in the black mat can be mainly attributed to the activity of SRB resulting in the production and precipita-

tion of iron sulphide minerals (Huerta-Diaz & Morse 1992; Watson et al. 1995; Beech & Cheung, 1995; Neumann et al. 2006). Studies showed that accumulations of TREE like Co, Cu, Mn and Ni with pyrite (FeS_2) are linear to the amount of pyrite produced, due to co-precipitation of these trace elements with biogenic pyrite (Huerta-Diaz & Morse 1992). Therefore, the TREE fractionation pattern observed in the black was related to the dominating SRB in this mat. Further comparison to TREE fractionation in SRB-derived iron sulphides is difficult due to sparse reference literature. In most contemporary palaeontological studies, the morphological occurrence (e.g., pyrite framboids) and or the fractionation of iron and sulphur isotopes is attributed to the activity of sulphate reducing prokaryotes (a.o., Beard et al. 1999; Icopini et al. 2004; Shen & Buik 2004; Fortin & Langley 2005; Watson et al. 2009; Canfield et al. 2010; Cavalazzi et al. 2012). However, a systematic evaluation of TREE fractionation in biogenic pyrite is necessary to allow a further differentiation from hydrothermal pyrite and its validation as a biosignature. As the white mat seem to consist of several dominating communities (sulphate reducing, sulphur oxidizing and methanotrophic bacteria) the TREE pattern of this mat will not be discussed further as clear attribution to a certain community is not possible.

Conclusions

Mineralizing microbial mats from an open pond in the subsurface were investigated. Although a visual differentiation of three different mat types (ochre, black and white) was possible, the microbial communities involved were much more complex and heterogeneous. However, a clear relation of a dominating microbial consortium to a respective mat type was partly possible, like the attribution of iron oxidizing bacteria to the ochre and sulphate reducing bacteria to the black mat. The microbial community of the white mat was rather complex and, unlike the other microbial mats, showed no indication for a clearly dominating metabolic group of microorganisms.

A clear relationship of between microbial key players and specific biogeochemical processes is necessary to evaluate microbially induced trace and rare earth element (TREE) accumulation and fractionation. These accumulation or fractionation patterns could therefore serve as potential biosignatures for the respective mat metabolism. The ochre mat dominated by iron oxidizing bacteria, showed an even 1000 fold accumulation of rare earth elements (REE), but still reflected the pattern of the feeder fluid. A similar behaviour is observed for the most higher valent trace metals that co-precipitated with the microbial iron oxyhydroxides. Therefore, the TREE enrichment pattern of the iron oxidizing microbial mat largely reflects the environmental conditions prevailing throughout the activity of the microbial mat. In contrast, the black mat, dominated by sulphate reducing bacteria, showed a TREE fractionation that significantly differs from both, the iron oxidizing microbial mat and the pond water. The accumulated TREE can mainly be attributed to the microbially formed pyrite within this mat. These observations point at a potential utility of this fraction pattern as a distinctive biosignature, but a further validation and comparison with other microbial mats and biotically and abiotically formed pyrites is necessary.

Acknowledgements

We thank two anonymous reviewers for their positive and constructive comments. In addition, we are grateful to the SKB staff for technical, logistic and analytical support at the Äspö HRL. Erwin Schiffzyk, and Dorothea Hause-Reitner are acknowledged for their assistance with the XRD, ICP-OES, and SEM-EDX measurements, respectively. Joachim Reitner is acknowledged for the initiation of this interesting project 'Biomineralisation, Biogeochemistry and Biodiversity of chemolithotrophic Microorganisms in the Tunnel of Äspö (Sweden)' within the frame of and funded by the DFG (German Research Foundation) research unit FOR 571. This is publication no. 65 of the DFG Research Unit FOR 571 'Geobiology of Organo- and Biofilms'.

References

Altschul, S. F.; Gish, W.; Miller, W.; Myers, E. W. & Lipman, D. J. (1990): Basic local alignment search tool. *Journal of Molecular Biology* **215**: 403-410. http://dx.doi.org/10.1016/S0022-2836(05)80360-2

Amann, R. I.; Krumholz, L. & Stahl, D. A. (1990): Fluorescent-oligonucleotide probing of whole cells for determinative, phylogenetic, and environmental studies in microbiology. *Journal of Bacteriology* **172**(2): 762-770.

Anderson, C. R. & Pedersen, K. (2003): *In situ* growth of *Gallionella* biofilms and partitioning of lanthanides and actinides between biological material and ferric oxyhydroxides. *Gebiology* **1**: 169-178. http://dx.doi.org/10.1046/j.1472-4669.2003.00013.x

Bailey, J. V.; Orphan, V. J.; Joye, S. B. & Corsetti, F. A. (2009): Chemotrophic Microbial Mats and Their Potential for preservation in the Rock Record. *Astrobiology* **9** (9): 843-859. http://dx.doi.org/10.1089/ast.2008.0314

Bau, M. (1999) Scavenging of dissolved yttrium and rare earths by precipitating iron oxyhydroxide: Experimental evidence for Ce oxidation, Y-Ho fractionation, and lanthanide tetrade effect. *Geochimica et Cosmochimica Acta* **63** (1): 67-77. http://dx.doi.org/10.1016/S0016-7037(99)00014-9

Bazylinski, D. A.; Frankel, R. B. & Konhauser, K. O. (2007): Modes of Biomineralization of Magnetite by Microbes. *Geomicrobiology Journal* **24** (6): 465-475. http://dx.doi.org/10.1080/01490450701572259

Beard, B. L.; Johnson, C. M.; Cox, L.; Sun, H.; Nealson, K. H. & Aguilar, C. (1999): Iron isotope biosignatures. *Science* **285** (5435): 1889-1892. http://dx.doi.org/10.1126/science.285.5435.1889

Camarini, G. & De Milito, J. A. (2011): Gypsum hemihydrate–cement blends to improve rendering durability. *Construction and Building Material* **25** (11): 4121-4125. http://dx.doi.org/10.1016/j.conbuildmat.2011.04.048

Canfield, D.; Farquhar, J. & Zerkle, A. L. (2010) High isotope fractionations during sulfate reduction in a low-sulfate euxinic

ocean analog. *Geology* **38** (5): 415-418. http://dx.doi.org/10.1130/G30723.1

Casamayor, E. O.; Schäfer, H.; Bañeras, L.; Pedrós-Alió, C. & Muyzer, G. (2000): Identification of and Spatio-Temporal Differences between Microbial Assemblages from Two Neighboring Sulfurous Lakes: Comparison by Microscopy and Denaturing Gradient Gel Electrophoresis. *Applied Environmental Microbiology* **66** (2): 499-508.

Cavalazzi, B.; Barbieri, R.; Cady, S. L.; George, A. D.; Gennaro, S.; Westall, F.; Luif, A.; Canteri, R.; Rossi, A. P.; Ori, G. G. & Taj-Eddie, K. (2012): Iron-framboids in the hydrocarbon-related Middle Devonian Hollard Mound of the Anti-Atlas mountain range in Morocco: Evidence of potential microbial biosignatures. *Sedimentary Geology* **263-264**:183-193. http://dx.doi.org/10.1016/j.sedgeo.2011.09.007

Chan, C. S.; Fakra, S. C.; Emerson, D.; Fleming, E. J. & Edwards K. J. (2011): Lithotrophic iron-oxidizing bacteria produce organic stalks to control mineral growth: implications for biosignature formation. *The ISME Journal* **5** (4): 717-727. http://dx.doi.org/10.1038/ismej.2010.173

Cholodny, N. G. (1926): Die Eisenbakterien - Beiträge zu einer Monographie. In: Kolkwitz, R. (ed.): *Pflanzenforschung* **4**. Jena (G. Fischer): vi + 162 pp.

Comolli, L. R.; Luef, B. & Chan, C. S. (2011): High-resolution 2D and 3D cryo-TEM reveals structural adaptations of two stalk-forming bacteria to an Fe-oxidizing lifestyle. *Environmental Microbiology* **13** (11): 2915-2929. http://dx.doi.org/10.1111/j.1462-2920.2011.02567.x

Cornell, M. & Schwertmann, U. (2004): *The Iron Oxides*. Weinheim (Wiley-VCH): 664 pp.

Daims, H.; Bruhl, A.; Amann, R.; Schleifer, K. H.; & Wagner, M. (1999): The domain-specific probe EUB338 is insufficient for the detection of all Bacteria: development and evaluation of a more comprehensive probe set. *Systematic and Applied Microbiology* **22**: 434-444. http://dx.doi.org/10.1016/S073-2020(99)80053-8

De Carlo, E. H.; Wen Xi-yuan & Irving, M. (1998): The Influence of Redox Reactions on the Uptake of Dissolved Ce by Suspended Fe and Mn Oxide Particles. *Aquatic Geochemistry* **3** (4): 357-389. http://dx.doi.org/10.1023/A:1009664626181

Emerson, D.; Flemming, E. J. & McBeth, J. M. (2010): Iron-Oxidizing Bacteria: An Environmental and Genomic Perspective. *Annual Reviews in Microbiology* **64**: 561-583. http://dx.doi.org/10.1146/annurev.micro.112408.134208

Emerson, D.; Rentz, J. A.; Lilburn, T. G.; Davis, R. E.; Aldrich, H.; Chan, C. & Moyer, C. L. (2007): A Novel Lineage of Proteobacteria Involved in Formation of Marine Fe-Oxidizing Microbial Mat Communities. *PLoS ONE* **2** (8): 1-9 [e667]. http://dx.doi.org/10.1371/journal.pone.0000667

Felsenstein, J. (1993): PHYLIP (Phylogeny Inference Package) version 3.5c. Distributed by the author. Department of Genetics, University of Washington, Seattle. (based on Felsenstein, J. 1989. PHYLIP -- Phylogeny Inference Package (Version 3.2). *Cladistics* **5**: 164-166. http://dx.doi.org/10.1111/j.1096-0031.1989.tb00562.x

Ferris, F. G.; Hallberg, R. O.; Lyvén, B. & Pedersen, K. (2000): Retention of strontium, cesium, lead and uranium by bacterial iron oxides from subterranean environment. *Applied Geochemistry* **15** (7): 1035-1042. http://dx.doi.org/10.1016/S0883-2927(99)00093-1

Ferris, F. G.; Kohnhauser, K. O.; Lyvén, B. & Pedersen, K. (1999): Accumulation of metals by bacteriogenic iron oxides in a subterranean environment. *Geomicrobiology Journal* **16** (2): 181-192. http://dx.doi.org/10.1080/014904599270677

Fortin, D.; Langley, S. (2005): Formation and occurrence of biogenic iron-rich minerals. *Earth-Science Reviews* **72**: 1-19. http://dx.doi.org/10.1016/j.earscirev.2005.03.002

Geets, J. B.; Borremans, L.; Diels, D.; Springael, J.; Vangronsveld, D.; Lelie, D. van der & Vanbroekhoven, K. (2006): DsrBgene-based DGGE for community and diversity surveys of sulfate-reducing bacteria. *Journal of Microbiology Methods* **66** (2):194-205. http://dx.doi.org/10.1016/j.mimet.2005.11.002

Guo, Xiao-lu & Shi, Hui-sheng (2008): Thermal treatment and utilization of flue gas desulphurization gypsum as an admixture in cement and concrete. *Construction and Building Materials* **22**: 1471-1476. http://dx.doi.org/10.1016/j.conbuildmat.2007.04.001

Haferburg, G. & Kothe, E. (2007): Microbes and metals: interactions in the environment. *Journal of Basic Microbiology* **47** (6): 453-467. http://dx.doi.org/10.1002/jobm.200700275

Haferburg, G.; Merten, D.; Büchel, G. & Kothe, E. (2007): Biosorption of metal and salt tolerant microbial isolates from a former uranium mining aerea. Their impact on changes in rare earth element patterns in acid mine drainage. *Journal of Basic Microbiology* **47** (6): 474-484.

Hall, T. A. (1999): BioEdit: a user-friendly biological sequence alignment editor and analysis program for Windows 95/98/NT. *Nucleic Acids Symposium Series* **41**: 95-98.

Hallbeck, L.; Ståhl, F. & Pedersen, K. (1993): Phylogeny and phenotypic characterization of the stalk-forming and iron-oxidizing bacterium *Gallionella ferruginea*. *Journal of General Microbiology* **139**:1531-1535. http://dx.doi.org/10.1099/00221287-139-7-1531

Hansen, H. P. (1999): Determination of oxygen. In: Grasshoff, K.; Kremling, K. & Ehrhardt, M. (eds.): *Methods of seawater analysis*. Hoboken (Wiley-VCH): 75-89.

Huerta-Diaz, M. A. & Morse J. W. (1992): Pyritization of trace metals in anoxic marine sediments. *Geochimica et Cosmochimica Acta* **56**: 2681-2702. http://dx.doi.org/10.1016/0016-7037(92)90353-K

Icopini, G. A.; Anbar, A. D.; Ruebush, S. S.; Tien, M. & Brantley, S. K. (2004): Iron isotope fractionation during microbial reduction of iron: The importance of adsorption. *Geology* **32** (3): 205-208. http://dx.doi.org/10.1130/G20184.1

Iglesias, J. G.; Álvarez, M. M. & Rodríguez, J. E. (1999): Influence of gypsum's mineralogical characteristics on its grinding behaviour applied to cement fabrication. *Cement and Concrete Research* **29** (5): 727-730. http://dx.doi.org/10.1016/S0008-8846(99)00038-1

Ionescu, D.; Siebert, C.; Munwes, Y. Y.; Lott, C.; Häusler, S.; Bizic-Ionescu, M.; Quast, C.; Peplies, J.; Glöckner, F. O.; Ramette, A.; Rödinger, T.; Dittmar, T.; Oren, A.; Geyer, S.; Stärk, H. J.; Sauter, M.; Licha, T.; Laronne, J. B. & De Beer, D. (2012): Microbial and Chemical Characterization of Underwater Fresh Water Springs in the Dead Sea. *PLoS ONE* **7** (6): 1-21 [e38319]. http://dx.doi.org/10.1371/journal.pone.0038319

Konhauser, K. O. (1997): Bacterial iron biomineralisation in nature. *FEMS Microbiology Reviews* **20** (3-4): 315-326. http://dx.doi.org/10.1016/S0168-6445(97)00014-4

Ludwig, W.; Strunk, O.; Westram, R.; Richter, L.; Meier, H.; Yadhukumar; Buchner, A.; Lai, T.; Steppi, S.; Jobb, G.; Förster, W.; Brettske, I.; Gerber, S.; Ginhart, A. W.; Gross, O.; Grumann, S.; Hermann, S.; Jost, R.; König, A.; Liss, T.; Lüßmann, R.; May, M.; Nonhoff, B.; Reichel, B.; Strehlow, R.; Stamatakis, A.; Stuckmann, N.; Vilbig, A.; Lenke, M.; Ludwig, T.; Bode, A. & Schleifer, K.-H. (2004): ARB: a software environment for sequence data. *Nucleic Acids Research* **32** (4): 1363-1371. http://dx.doi.org/10.1093/nar/gkh293

Mahmood, S.; Freitag, T. E. & Prosser, J. I. (2006): Comparison of PCR primer-based strategies for characterization of ammonia oxidizer communities in environmental samples. *FEMS Microbiology Ecology* **56** (3): 482-493. http://dx.doi.org/10.1111/j.1574-6941.2006.00080.x

Manz, W.; Amann, R.; Ludwig, W.; Wagner, M. & Schleifer, K. H. (1992): Phylogenetic Oligodeoxynucleotide Probes for the Major Subclasses of Proteobacteria: Problems and Solutions. *Systematic and Applied Microbiology* **15** (4): 593-600.

Manz, W.; Eisenbrecher, M.; Neu, T. R. & Szewzyk, U. (1998): Abundance and spatial organization of Gram-negative sulfate-reducing bacteria in activated sludge investigated by in situ probing with specific 16S rRNA targeted oligonucleotides. *FEMS Microbiology Ecology* **25** (1): 43-61. http://dx.doi.org/10.1111/j.1574-6941.1998.tb00459.x

Michel, M. F.; Ehm, L.; Antao, S. M.; Lee, P. L.; Chupas, P. J.; Liu, G.; Strongin, D. R.; Schoonen, M. A. A.; Phillips, B. L. & Parise, J. B. (2007): The structure of ferrihydrite, a nanocycrstalline material. *Science* **316** (5832): 1726-1729. http://dx.doi.org/10.1126/science.1142525

Muyzer, G.; Teske, A.; Wirsen, C. O. & Jannasch, H. W. (1995): Phylogenetic relationships of *Thiomicrospira* species and their identification in deep-sea hydrothermal vent samples by denaturing gradient gel electrophoresis of 16S rDNA fragments. *Archives of Microbiology* **164** (3):165-172. http://dx.doi.org/10.1007/BF02529967

Nikolausz, M.; Sipos, R.; Révész, S.; Székely, A. & Márialigeti, K. (2005): Observation of bias associated with re-amplification of DNA isolated from denaturing gradient gels. *FEMS Microbiology Letters* **244** (2): 385-390. http://dx.doi.org/10.1016/j.femsle.2005.02.013

Pedersen, K. (1997): Microbial life in deep granitic rock. *FEMS Microbiology Reviews* **20** (3-4): 399-414. http://dx.doi.org/10.1111/j.1574-6976.1997.tb00325.x

Pedersen K.; Arlinger, J.; Ekendahl, S. & Hallbeck, L. (1996): 16s rRNA gene diversity of attached and unattached bacteria in boreholes along the access tunnel to the Äspö Hard Rock Laboratory, Sweden. *FEMS Microbiology Ecology* **19**: 249-262. http://dx.doi.org/10.1111/j.1574-6941.1996.tb00217.x

Quast, C.; Pruesse, E.; Yilmaz, P.; Gerken, J.; Schweer, T.; Yarza, P.; Peplies, J. & Glöckner, F. O. (2013): The SILVA ribosomal RNA gene database project: improved data processing and web-based tools. *Nucleic acids research* **41** (Database issue): D590–6. http://dx.doi.org/10.1093/nar.gks1219

Reguera, G.; McCarthy, K. D.; Mehta, T.; Nicoll, J. S.; Tuominen, M. T. & Lovely, D. R. (2005): Extracellular electron transfer via microbial nanowires. *Nature* **435** (7045): 1098-1101. http://dx.doi.org/10.1038/nature03661

Russel, M. J. (2003): The importance of being alkaline. *Science* **302** (5645): 580-581. http://dx.doi.org/10.1126/science.1091765

Santegoeds, C. M.; Schramm, A. & de Beer, D. (1998): Microsensors as a tool to determine chemical microgradients and bacterial activity in wastewater biofilms and flocs. *Biodegradation* **9** (3-4): 159-167. http://dx.doi.org/10.1023/A:1008302622946

Schäfer, H. & Muyzer, G. (2001): Denaturing gradient gel electrophoresis in marine microbial ecology. *Methods in Microbiology* **30**: 425-468. http://dx.doi.org/10.1128/AEM.67.7.2942-2951.2001

Shen Yanan & Buick, R. (2004): The antiquity of microbial sulfate reduction. *Earth Science Reviews* **64** (3-4): 243-272. http://dx.doi.org/10.1016/S0012-8252(03)00054-0

Snaidr, J.; Amann, R.; Huber, I.; Ludwig, W. & Schleifer, K. H. (1997): Phylogenetic analysis and in situ identification of bacteria in activated sludge. *Applied Environmental Microbiology* **63** (7): 2884-2896.

Sorokin, D. Y.; Tourova, T. P. & Muyzer, G. (2005): *Citreicella thiooxidans* gen. nov., sp. nov., a novel lithoheterotrophic sulfur-oxidizing bacterium from the Black Sea. *Systematic and Applied Microbiology* **28** (8): 679-687. http://dx.doi.org/10.1016/j.syapm.2005.05.006

Straub, K. L.; Benz, M.; Schink, B. & Widdel, F. (1996): Anaerobic, nitrate-dependent microbial oxidation of ferrous iron. *Applied Environmental Microbiology* **62** (4): 1458-1460.

Takahashi, Y.; Hirata, T.; Shimizu, H.; Ozaki, T. & Fortin, D. (2007): A rare earth element signature of bacteria in natural waters? *Chemical Geology* **244** (3-4): 569-583. http://dx.doi.org/10.1016/j.chemgeo.2007.07.005

Templeton, A. & Knowles, E. (2009): Microbial Transformations of Minerals and Metals: Recent Advances in Geomicrobiology Derived from Synchrotron-Based X-Ray Spectroscopy and X-Ray Microscopy. *Annual Reviews in Earth and Planetary Sciences* **37**: 367-391. http://dx.doi.org/10.1146/annurev.earth.36.031207.124346

Trevors, J. T. (2002): The subsurface origin of microbial life on the Earth. *Research in Microbiology* **153** (8): 487-491. http://dx.doi.org/10.1016/S0923-2508(02)01360-8

Wagner, M. A.; Roger, J.; Flax, J. L.; Brusseau, G. A. & Stahl, D. A. (1998): Phylogeny of Dissimilatory Sulfite Reductases Supports an Early Origin of Sulfate Respiration. *Journal of Bacteriology* **180** (11): 2975-2982.

Wallner, G.; Amann, R.; Beisker, W. (1993): Optimizing fluorescent in situ hybridization with rRNA-targeted oligonucleotide probes for flow cytometric identification of microorganisms. *Cytometry* **14** (2): 136-143. http://dx.doi.org/10.1002/cyto.990140205

Watson, E. B.; Cherniak, D. J. & Frank, E. A. (2009): Retention of biosignatures and mass-independent fractionations in pyrite: Self-diffusion of sulfur. *Geochimica et Cosmochimica Acta* **73**: 4792-4802. http://dx.doi.org/10.1016/j.gca.2009.05.060

Weiner, S. & Dove, P. M. (2003): An Overview of Biomineralization Processes and the Problem of the Vital Effect. In: Dove, P. M.; De Yoreo, J. J. & Weiner, S. (eds.): Biomineralization. *Reviews in Mineralogy & Geochemistry* **54** (1): 1-29. http://dx.doi.org/10.2113/0540001

Wieland, A.; Zopfi, J.; Benthien, M. & Kühl, M. (2005) Biogeochemistry of an Iron-Rich Hypersaline Microbial Mat (Camargue, France). *Microbial Ecology* **49** (1): 34-49. http://dx.doi.org/10.1007/s00248-003-2033-4

Cite this article: Heim, C.; Quéric, N.-V.; Ionescu, D.; Simon, K. & Thiel, V. (2014): Chemolithotrophic microbial mats in an open pond in the continental subsurface – implications for microbial biosignatures. *In:* Wiese, F.; Reich, M. & Arp, G. (eds.): "Spongy, slimy, cosy & more…". Commemorative volume in celebration of the 60th birthday of Joachim Reitner. *Göttingen Contributions to Geosciences* **77**: 99–112.

http://dx.doi.org/10.3249/webdoc-3921